# Algorithms, performance, development of the ATLAS High-Level trigger

**Kunihiro Nagano**
**on behalf of the ATLAS Collaboration**

Associate Professor, High Energy Research Organization (KEK), 1-1 Oho, Tsukuba, Ibaraki, Japan

E-mail: kunihiro.nagano@cern.ch

**Abstract.** The ATLAS trigger system has been used for the online event selection for three years of LHC data-taking and is preparing for the next run. The trigger system consists of a hardware level-1 and a software high-level trigger (HLT) which is implemented in a region-of-interest based level-2 stage and a event filter operating after event building with offline-like software. During the past three years, the luminosity and pile-up (number of collisions per beam crossing) has increased significantly placing escalating demands on the rejection and timing performance. The HLT algorithms advanced during this period to maintain and even improve performance. Also discussed is the work towards the merging of the two HLT levels in to a single level HLT.

ATL-DAQ-PROC-2014-001
20/01/2014

## 1. Introduction

The Large Hadron Collider (LHC) is currently the highest energy proton-proton ($p$-$p$) collider, and searches for new particles or phenomena at the energy frontier. In addition, it also provides precision measurements of standard model processes. The long-sought Higgs boson was discovered from the three years of LHC data (called Run1).

The ATLAS experiment collected $p$-$p$ collision data in 2012 (2011) at a center-of-mass energy of 8 (7) TeV with a maximum instantaneous luminosity of $7.7(3.65) \cdot 10^{33}$ cm$^{-2}$ s$^{-1}$. Due to the small cross sections of these interesting signals compared to the huge $p$-$p$ scattering cross section, a large rejection is necessary at trigger level (about a factor 5000 in 2012). In addition, many collisions occur in each bunch crossing (called in-time pile-up collisions), and the trigger needs to maintain the performance in such harsh conditions. This report discusses the algorithms, performance, and ongoing development work on the reconstruction of calorimeter objects, inner detector tracking, and muon reconstruction in the ATLAS trigger.

## 2. ATLAS Detector and Trigger

The ATLAS detector is a multipurpose particle physics apparatus consisting of four major sub-systems, the inner detector (ID), electromagnetic calorimeter, hadronic calorimeter and muon spectrometer (MS). A detailed description of the ATLAS detector can be found elsewhere [1].

The ATLAS trigger system has three levels; the first level (L1) is a hardware-based system using information from the calorimeter and muon sub-detectors, the second (L2) and third (Event Filter, EF) levels are software-based systems using information from all sub-detectors.

Together, L2 and EF are called the High Level Trigger (HLT). The triggers are based on identifying combinations of candidate physics objects such as electrons, photons, muons, jets, jets with $b$-flavor tagging ($b$-jets) as well as global event properties such as missing transverse energy ($E_T^{\mathrm{miss}}$) and summed transverse energy ($\Sigma E_T$).

In 2012, the typical maximum L1 rate was 70 kHz. In addition to performing the first selection step, the L1 triggers identify Regions of Interest (RoIs) within the detector to be investigated by the HLT. The L2 selection is based on fast custom algorithms processing partial event data within the RoIs. In 2012, the L2 triggers reduce the rate typically to 5 kHz with an average processing time of 75 ms/event. The EF selection is mostly based on offline algorithms and is provided with full event information assembled by the Event Builder. In 2012, the EF reduced the rate to 700 Hz on average (with peaks of about 1 kHz) with an average processing time of 1 s/event. Data are written to inclusive data streams based on the trigger type. Figure 1

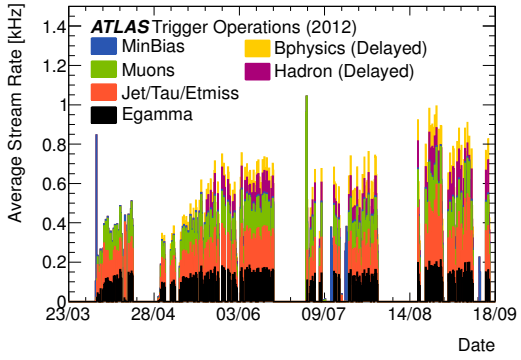


**Figure 1.** EF recording rates in 2012, separately for data streams [2]. There are four primary physics streams, Egamma, Muons, JetTauEtmiss, MinBias, plus two delayed physics streams, Bphysics and Hadron.

shows the recording rates in 2012 runs separately for each data stream. The trigger system is configured via a trigger menu which defines trigger chains that start from an L1 trigger and specify a sequence of reconstruction and selection steps for the specific trigger signatures required in the trigger chain. Approximately 500 trigger chains are defined in the trigger menus which are composed of a number of different classes of trigger: single object triggers, multiple object triggers, combined triggers (with two or more characteristic objects of different types), as well as supporting triggers, for example for background estimations and for in-situ performance measurements. Only three trigger menus were used in Run1 (two in 2011 and one in 2012), avoiding complications in physics analysis due to frequent trigger changes.

## 3. Muon trigger

Muons are triggered at L1 using the RPC system in the barrel region ($|\eta| < 1.05$) and the TGC system in the end-cap regions ($1.05 < |\eta| < 2.4$). At L2, the candidate from L1 is first refined by using the data from MS precision chambers, which are then combined with the tracks found in the ID. The EF muon reconstruction has two algorithms; one is the "outside-in" strategy of forming a muon candidate using MS information first to combine to an ID track, the other is the "inside-out" strategy of starting with ID tracks and extrapolating them to the MS to form a muon candidate. These two strategies were used in parallel until the end of the 2011 run, but from 2012 onward the "outside-in" algorithm is run first and is subsequently complemented by the "inside-out" algorithm, only if the first fails. More details can be found in Refs. [3, 4].

The single muon trigger is widely used in many physics analyses. The $p_T$ threshold for the single muon trigger was 18 GeV in 2011, and was raised to 24 GeV in 2012; in addition an isolation requirement was added as $\Sigma^{\Delta R<0.2} p_T^{\mathrm{trk}}/p_{T,\mu} < 0.12$, where $p_{T,\mu}$ is the $p_T$ of the muon and $\Sigma^{\Delta R<0.2} p_T^{\mathrm{trk}}$ is the sum of $p_T$ of ID tracks in a cone of $\Delta R = \sqrt{(\Delta\phi)^2 + (\Delta\eta)^2} < 0.2$ centered

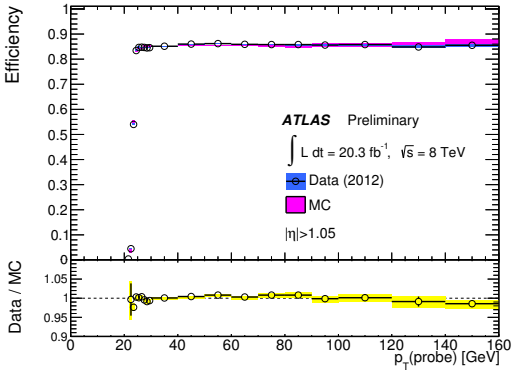


**Figure 2.** Single muon trigger efficiency as a function of $p_T$ in the endcap region, $|\eta| > 1.05$ [5].

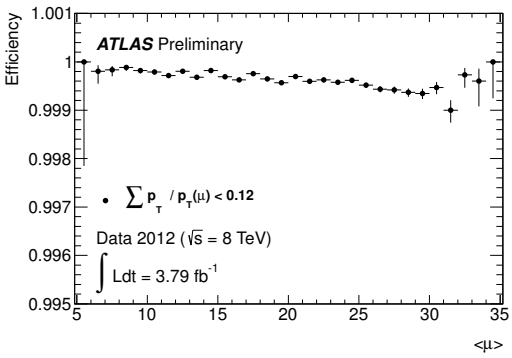


**Figure 3.** Single muon trigger efficiency as a function of average number of interactions per bunch crossing, $< \mu >$ [5].

around the muon after subtracting the $p_T$ of the muon itself. Figure 2 shows the efficiency of the single muon trigger as a function of muon $p_T$. The efficiency is about 86 (70)% at plateau in the endcap (barrel) region, mostly due to the limited L1 detector geometric coverage. Figure 3 shows the efficiency of the isolation requirement in the single muon trigger as a function of the average number of interactions per bunch crossing, $< \mu >$. The efficiency is defined with respect to isolated offline muons. It is shown that the isolation requirement is robust against pile-up.

The threshold for the di-muon trigger was 10 GeV in 2011, which was raised to 13 GeV in 2012. In addition, an asymmetric di-muon trigger with $p_T > 18, 8$ GeV was introduced in 2012 by utilizing muon finding that scans the full detector at EF to find a second muon ($p_T > 8$ GeV) after first muon is found by usual RoI-based trigger. This increased efficiency by recovering L1 geometrical inefficiency.

## 4. Electron and photon trigger

At L1, $e/\gamma$ clusters are triggered using calorimeter information from reduced-granularity signals, called Trigger Towers (TT), each covering $\Delta\eta \times \Delta\phi \approx 0.1 \times 0.1$. The L2 $e/\gamma$-triggers perform a fast calorimeter reconstruction algorithm, and in the case of electrons, a fast inner detector track reconstruction. The cluster reconstruction and the track reconstruction at the EF is performed as in the offline. More details can be found in Ref. [6].

For 2012 runs, the electron identification cuts were optimized for anticipated large pile-up; cuts on pile-up sensitive quantities, typically radial shower size, were loosened. The $p_T$ threshold for the single electron trigger was 22 GeV in 2011, and was raised to 24 GeV in 2012; in addition an isolation requirement was added as $\Sigma^{\Delta R<0.2} p_T^{trk}/E_{T,e} < 0.10$, which is defined similarly to the isolation used in the muon trigger, and where $E_{T,e}$ is the transverse energy of the electron candidate. Figure 4 shows the efficiency of the single electron trigger as a function of electron $E_T$. The efficiency was about 95% at plateau. An additional 2 – 3% efficiency is recovered at high $E_T$ by removing the isolation requirement for $E_T > 60$ GeV. Figure 5 shows the efficiency of the single electron trigger as a function of number of vertices in event. It is seen that there is almost no dependence on pile-up. The threshold for di-electron trigger was 10 GeV in 2011, which was raised to 12 GeV in 2012.

The cuts for photon identification were also optimized for pile-up similar to the electron cuts. As the diphoton trigger is essential for a Higgs boson decaying to two photons, the thresholds were kept low $E_T > 30, 20$ GeV in both years, and the photon identification cuts were only

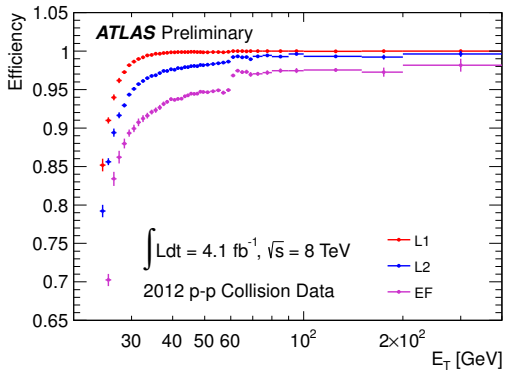


**Figure 4.** Single electron trigger efficiency as a function of electron $E_T$, separately for L1, L2, EF levels [7].

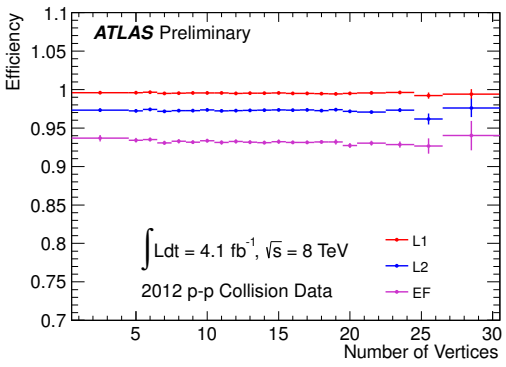


**Figure 5.** Single electron trigger efficiency as a function of number of vertices in event, separately for L1, L2, EF levels [7].

slightly tightened in 2012. For the single photon trigger, the threshold was raised to 120 GeV in 2012. The efficiency of the photon trigger is about 100% at plateau.

## 5. Hadronic tau trigger

At L1, the tau trigger uses electromagnetic and hadronic calorimeter TTs to calculate energy in a core region and an isolation region around the core. At L2, selection criteria are applied by requiring narrowness and low track multiplicity to discriminate taus from the multi-jet background. In 2012, the pile-up robustness of the L2 selection was largely improved by removing pile-up sensitive variables and by reducing calorimeter cone size. At EF, two multivariate (MV) algorithms were implemented in 2012: a Boosted Decision Tree and a Log Likelihood. The MV algorithms are given pile-up robust variables as input, with working points defined separately for one and multi-prong tau candidates.

The tau triggers are mostly used in combination with a second tau (which is either a hadronic or leptonic decay) or missing transverse energy. They are crucial for example for Higgs decaying to two taus and SUSY searches. Figure 6 shows the efficiency as a function of tau $p_T$, and Figure 7 shows the efficiency as a function of number of vertices in event. The efficiencies are in

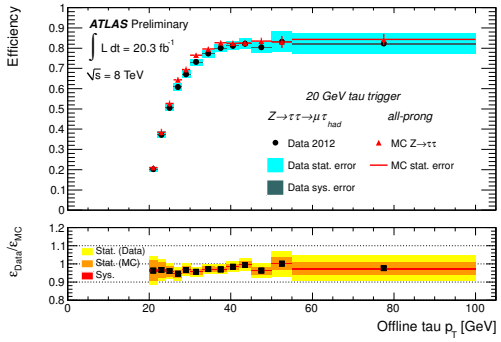


**Figure 6.** Tau trigger efficiency as a function of tau $p_T$ [8].

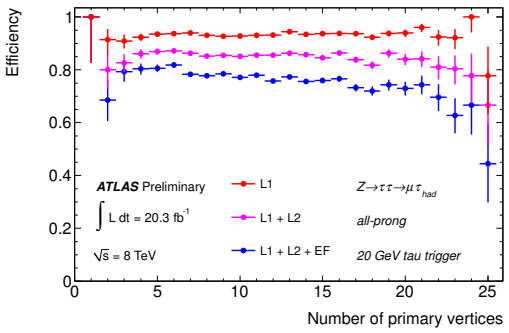


**Figure 7.** Tau trigger efficiency as a function of number of vertices in event [8].

good agreement with the simulation, and are robust against pile-up. More details can be found in Refs. [9, 10].

## 6. Jet trigger

Jet trigger has undergone substantial modifications, the RoI-based strategy has been replaced by a full scan of the calorimeter data at the EF. Also for the L2 in 2012, a full scan (L2FS) using all TTs produced by the L1 in an anti-k$_T$ algorithm was made. Figure 8 shows the efficiency for

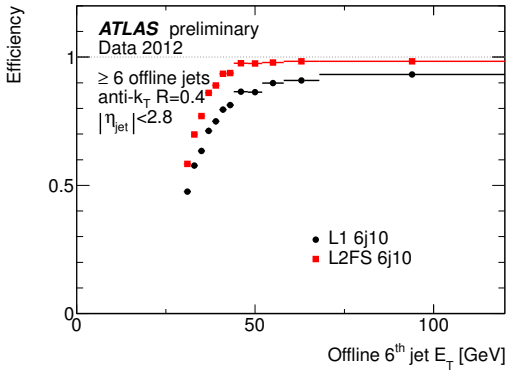


**Figure 8.** Efficiency for L1 and L2FS jets to satisfy a six jet trigger, as a function of the sixth offline jet $E_T$ [11].

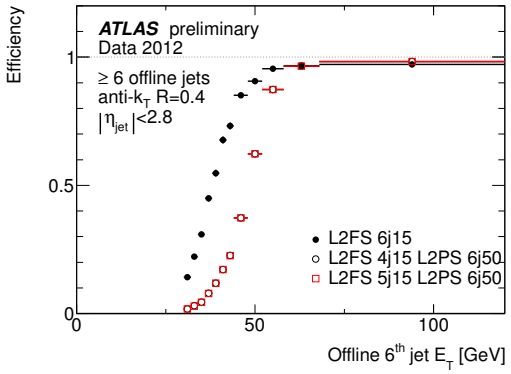


**Figure 9.** Efficiency for L2FS and L2PS jets to satisfy a six jet trigger, as a function of the sixth offline jet $E_T$ [11].

L1 and L2FS jets to satisfy a six jet trigger in events where at least six jets have been identified offline. It is seen that the L2 FS implementation improves the efficiency for multijet events.

From 2011, only calorimeter cells with energy depositions above a certain threshold (depending on pile-up conditions) are considered at HLT in order to mitigate noise and pile-up effects. This suppression gives improved jet energy resolution and hence sharpened efficiency turn-on. In addition, an L2 partial scan (L2PS) was developed; L2PS jets are built by running anti-k$_T$ algorithm on the calorimeter cells only from regions where significant jet activity was found by the L2FS. Figure 9 shows the efficiency for L2FS and L2PS jets to satisfy a six jet trigger. The better resolution of calorimeter cells (L2PS) with respect to L1-calorimeter towers (L2FS) allows for more efficient rejection. More details can be found in Ref. [12].

### *6.1. b-jet trigger*

Since 2012, a more advanced $b$-tagging was implemented at EF, which combines an impact-parameter (IP) based and secondary vertex (SV) finding based algorithms. These utilize a likelihood of the transverse and longitudinal IP distributions and a likelihood of secondary vertex reconstruction for instance mass, number of two-track vertices and the fraction of energy in the SV, to give a combined weight. Figure 10 shows the distribution of the weights given by the EF $b$-tagging algorithm. It improved 4-5 times the rejection of non-$b$-jets. More details can be found in Ref. [14].

## 7. Missing energy trigger

At L1, the TTs are used to compute both the $\Sigma E_T$ and $E_T^{\text{miss}}$ summing over the full ATLAS acceptance ($|\eta| < 4.9$). The noise threshold at L1 was optimized per tower; pile-up effectively increases noises, particularly in the forward calorimeter. The effect on resolution is small,

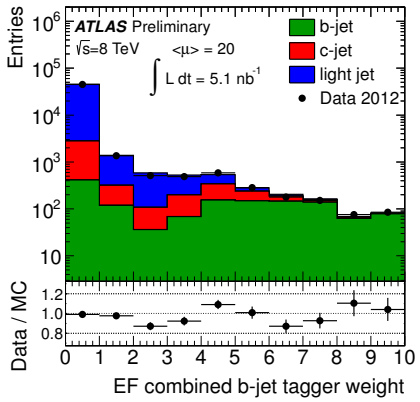


**Figure 10.** Distribution of the weight by the EF $b$-jet algorithm [13].

however the trigger rates were significantly reduced. Also, the first 3 bunch-crossings in a bunch train were vetoed in some triggers to further lower the threshold. These bunches have a different effective threshold because of the lack of out-of-time pile-up, which is expected by the electronics shaping, preceding them.

At L2, a significant improvement was made. Up to 2011, the L2 was almost same as L1, as the RoI scheme gives little benefit to global quantities such as $E_T^{\rm miss}$. Then, a new L2 algorithm which makes use of the special summary data stored in calorimeter front-end-buffer to calculate $E_T^{\rm miss}$ was implemented (L2 FEB). The resolution was improved by about 50%, as shown in Figure 11.

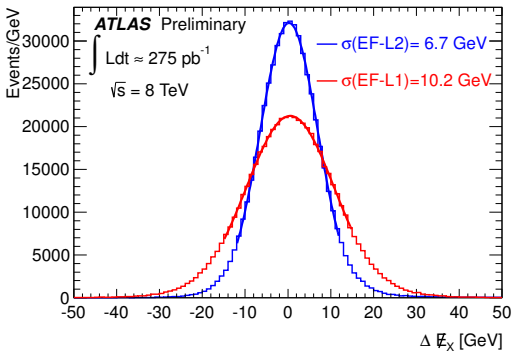


**Figure 11.** L1 and L2 FEB $E_T^{\rm miss}$ resolutions with respect to EF [15].

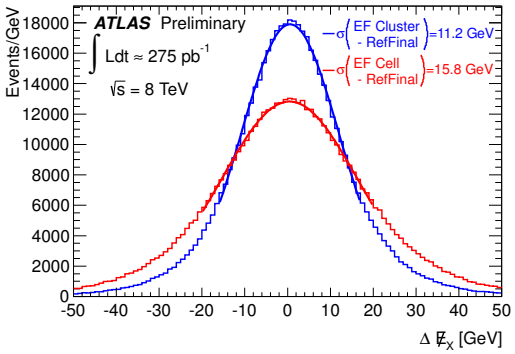


**Figure 12.** EF $E_T^{\rm miss}$ resolutions with respect to the offline quantity [15]. Separately shown for different clustering algorithms to EF $E_T^{\rm miss}$ calculation.

At EF, full granularity of the detectors is used for both calorimeters. The $\Sigma E_T$ and $E_T^{\rm miss}$ are calculated by summing over all calorimeter cells. A cluster-based calculation of $E_T^{\rm miss}$ and hadronic calibration were introduced, which improved resolution by about 40%, as in Figure 12.

## 8. Development towards Run2

LHC is planned to resume its operation from 2015 with increased energy and luminosity (called Run2). The physics goals in Run2 require triggers with similar $p_T$ thresholds as in Run1. In particular, for precision measurements of Higgs in various production and decay channels. As

cross sections grow by about a factor of two due to increased collision energy and the luminosity grows by about a factor of three, this implies that the demand on trigger grows significantly. The most severe constraint is L1. Ongoing work will extend the L1 limit to 100 kHz. Also, a topological processor (L1Topo) between object candidates found by the L1 will be implemented for Run2, which is expected to aid in maintaining low thresholds by introducing cuts on angular information in addition to thresholds. Also, HLT needs significant improvements, for instance, speeding up algorithm to overcome the increase of computing time due to high pile-up and higher L1 input rates. Among many improvements foreseen, the Fast Tracker (FTK) and merged HLT schema are briefly described in the following.

The FTK will receive data from the ID sub-detectors after each L1 trigger, and will provide full detector tracking. It is expected to provide an improved $b$-tagging and tau identification. Also, FTK tracks can be used to seed HLT tracking to speed up the net computing time. In the new merged HLT schema, former L2 and EF algorithms run in one processor. As the limitation on network transfer of data from L2 to EF algorithms is removed, it is expected that EF algorithms can make full use of L2 calculations and also data access can be minimized. In addition, the new schema allows a flexible event building. More details can be found in Refs. [16, 17].

## 9. Summary

The ATLAS trigger operated successfully in Run1. The efficiency loss due to trigger is typically a few %, and the efficiencies are accurately measured using data. Many new improvements in trigger were successfully made, which preserves and even improves trigger efficiency for various physics targets. For instance in the missing transverse energy trigger, L1/L2 thresholds were even lowered in 2012. Development for Run2 is on-going. Many changes are planned to cope with challenging conditions.

## References


[1] ATLAS Collaboration 2008 *Journal of Instrumentation* **3, S08003** 1–437
[2] ATLAS Collaboration *https://twiki.cern.ch/twiki/bin/view/AtlasPublic/TriggerOperationPublicResults*
[3] ATLAS Collaboration *Performance of the ATLAS muon trigger in 2011* (ATLAS-CONF-2012-099; https://cds.cern.ch/record/1462601)
[4] M Woudstra *Contribution to this proceedings*
[5] ATLAS Collaboration *https://twiki.cern.ch/twiki/bin/view/AtlasPublic/MuonTriggerPublicResults*
[6] ATLAS Collaboration *Performance of the Electron and Photon Trigger in p-p Collisions at* $\sqrt{s} = 7$ *TeV with the ATLAS Detector at the LHC in 2011* (ATLAS-CONF-2012-048; https://cds.cern.ch/record/1450089)
[7] ATLAS Collaboration *https://twiki.cern.ch/twiki/bin/view/AtlasPublic/EgammaTriggerPublicResults*
[8] ATLAS Collaboration *https://twiki.cern.ch/twiki/bin/view/AtlasPublic/TauTriggerPublicResults*
[9] ATLAS Collaboration *Performance of the ATLAS tau trigger in 2011* (ATLAS-CONF-2013-006; https://cds.cern.ch/record/1510157)
[10] J Mahlstedt *Contribution to this proceedings*
[11] ATLAS Collaboration *https://twiki.cern.ch/twiki/bin/view/AtlasPublic/JetTriggerPublicResults*
[12] S Shimizu *Contribution to this proceedings*
[13] ATLAS Collaboration *https://twiki.cern.ch/twiki/bin/view/AtlasPublic/BjetTriggerPublicResults*
[14] A Buzatu *Contribution to this proceedings*
[15] ATLAS Collaboration *https://twiki.cern.ch/twiki/bin/view/AtlasPublic/MissingEtTriggerPublicResults*
[16] N Garelli *Contribution to this proceedings*
[17] T Bold *Contribution to this proceedings*